

Microwave assisted gating of spin wave propagation

Cite as: Appl. Phys. Lett. **116**, 162403 (2020); <https://doi.org/10.1063/5.0006945>

Submitted: 07 March 2020 • Accepted: 05 April 2020 • Published Online: 21 April 2020

 Arabinda Haldar and  Adekunle Olusola Adeyeye



View Online



Export Citation



CrossMark

ARTICLES YOU MAY BE INTERESTED IN

[Introduction to spin wave computing](#)

Journal of Applied Physics **128**, 161101 (2020); <https://doi.org/10.1063/5.0019328>

[The design and verification of MuMax3](#)

AIP Advances **4**, 107133 (2014); <https://doi.org/10.1063/1.4899186>


[Spin-orbit-torque magnonics](#)

Journal of Applied Physics **127**, 170901 (2020); <https://doi.org/10.1063/5.0007095>

 Lake Shore
CRYOTRONICS



240 Series Sensor Input Modules

For precision cryogenic temperature monitoring over PLC networks [LEARN MORE](#) 

Microwave assisted gating of spin wave propagation

Cite as: Appl. Phys. Lett. **116**, 162403 (2020); doi: [10.1063/5.0006945](https://doi.org/10.1063/5.0006945)

Submitted: 7 March 2020 · Accepted: 5 April 2020 ·

Published Online: 21 April 2020



View Online



Export Citation



CrossMark

Arabinda Haldar^{1,2,a)}  and Adekunle Olusola Adeyeye^{2,3} 

AFFILIATIONS

¹Department of Physics, Indian Institute of Technology Hyderabad, Kandi 502285, Telangana, India

²Department of Electrical and Computer Engineering, National University of Singapore, Singapore 11757, Singapore

³Department of Physics, Durham University, South Road, Durham DH1 3LE, United Kingdom

^{a)} Author to whom correspondence should be addressed: arabinda@phy.iith.ac.in

ABSTRACT

Magnonics is an emerging research area where magnons or spin waves are used as a medium of information processing. Efficient manipulation/gating of magnons on-chip is crucial for realization of logic circuitry and device integration. Here, we show a simple method for gating of the magnons in a magnetic wire based on the dipolar coupled chain of nanomagnets. Spin wave propagation has been directly measured using the micro-Brillouin light scattering technique. We observed a significant reduction of spin wave amplitude by switching the nanomagnets using microwave current through a coplanar waveguide, which was also used for spin wave generation. Microwave assisted magnetization switching has been probed using the magnetic force microscopy technique. The results have potential implications in the area of wave based devices for next generation high frequency communication technologies.

Published under license by AIP Publishing. <https://doi.org/10.1063/5.0006945>

With the increasing demand for high speed, large bandwidth, and parallel data processing, alternatives to current CMOS (charge coupled metal oxide semiconductor) based technologies are of great demand.¹ In this regard, magnonics is poised to play a significant role where magnons are used for information transfer.^{2–4} Magnons are the quanta for spin waves (SWs), which are solid state coherent excitations in a magnetically ordered material. Spin wave propagation or magnon current does not require any movement of the electrons and thus can also propagate through insulators in addition to metallic magnetic materials. The frequencies of the magnons are in the range of few GHz to few-100 GHz and thus offer a great opportunity for exploring the huge microwave spectrum, which is mostly unused in current communication technologies. Similar to a CMOS transistor, a magnonic transistor consists of a source, drain, and gate, which generate, detect, and manipulate the magnon current, respectively.⁵ Demonstrations of magnon current generation using spin-transfer torque^{6,7} (charge current to magnon current conversion) and detection of magnon current using the inverse spin Hall effect (magnon current to charge current conversion) offer this wave based data processing technology for on-chip device integration. Gating operation, which is a crucial part of any device and also a subject of this report, has been achieved in several ways for creating magnonic logic circuitry. One of the first demonstrations is based on current controlled phase shifters in a

Mach-Zender type interferometer where the amplitude of the magnon current is monitored.^{8–10} Owing to inherent wave properties, the phase of the magnons is also used for data processing, which offers additional degrees of freedom, enabling a route for parallel data processing.^{11,12} All magnonic transistors have been shown recently where a magnon is manipulated with another magnon through non-linear magnon-magnon scattering processes.¹³ A reconfigurable and fabrication free gating operation is shown by using tunable laser induced thermal patterns that create variations in local magnetizations due to heating.¹⁴ Propagation of magnons through domain walls and their control are demonstrated by using a small external field¹⁵ and fully reconfigurable thermally assisted scanning probe lithography.¹⁶ Magnonic crystals are found to have spin wave dispersions based on different magnetic ordering, which can be reconfigured on demand.¹⁷

Recently, we have demonstrated spin wave propagation in a magnetic wire, which is based on a dipolar coupled but physically separated chain of rhomboid shaped nanomagnets that have unique magnetic states at remanence based on the field initializations along short or hard axes.¹⁸ Rhomboid shaped nanomagnets are quite different with respect to a rectangular nanomagnet in terms of their remanent magnetic states when an initialization field is applied along the short axis of the nanomagnet.¹⁹ Such shape engineered structures are

found to be interesting for tunable microwave operation and spin wave (SW) propagation without a bias magnetic field. Gating of spin waves was earlier achieved by switching a nanomagnet in the nanowire by applying an external magnetic field on a strategically fabricated nanowire with a “defect.” Nanowires with three different defect positions were lithographically fabricated in order to demonstrate the gating operation. Such a switching process would require an additional current line (Oersted field) to switch a nanomagnet on the magnetic wire for on-chip gating of spin waves.

In the present work, we demonstrate a method for gating of spin waves using microwave current, which reduces the number of lithographic fabrication processes. We have utilized a similar magnetic wire as used in our earlier report.¹⁸ A coplanar waveguide (CPW) was used for applying the microwave current. Generation and gating of spin waves are achieved using the same CPW. We have monitored the amplitude of the spin waves at a location away from the CPW using the micro-Brillouin light scattering (micro-BLS) technique. Spin wave intensity is found to be significantly reduced by 2.5 times after the gating operation using high power microwave current. Magnetic states are directly probed using the magnetic force microscopy (MFM) technique. These results offer less complex magnonic circuitry for practical realizations of magnonic devices.

The schematic of the micro-BLS experimental setup is shown in Fig. 1(a) in order to probe spin waves. Micro-BLS is the best-known tool for nanoscale spatial imaging of the spin waves. In this technique, a monochromatic laser is focused by using a large numerical aperture (N.A. = 0.75) microscope objective ($\times 100$) down to a diffraction limited spot diameter of around 300 nm. The scattered laser beam from the sample is analyzed by using a six-pass tandem Fabry-Pérot interferometer. The sample is placed on top of a nanostage that can be moved in 10 nm steps along x- and y-directions. In order to monitor the laser focusing over time, the z-axis of the nanostage is controlled

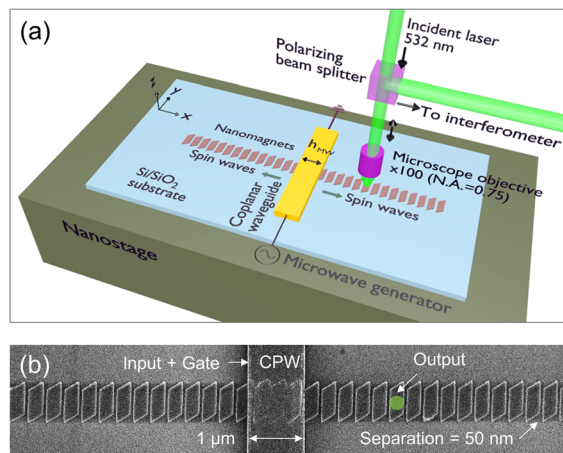


FIG. 1. (a) Schematic of the micro-BLS experiment where spin waves are excited in the sample with microwave current using a coplanar waveguide (CPW). The magnetic nanowire sample is placed on a nanostage to carry out raster scanning under the focused laser spot. (b) SEM image of the nanowire based on dipolar coupled but physically isolated rhomboid nanomagnets. The width of the CPW is $1\ \mu\text{m}$. The microwave field is denoted by h_{MW} . The output signal is measured at the position of the circular dot. CPW is used as an input and a gate to excite and gate spin waves, respectively.

through a feedback loop mechanism. The sample position and setting of the scan area can be performed by using a CCD camera and white light arrangement in a collinear geometry. The whole measurement setup is controlled remotely using commercial computer controlled software. More details of the micro-BLS technique can be found elsewhere.^{20,21} We have created a magnetic nanowire based on physically isolated rhomboid nanomagnets. In order to ensure dipolar coupling between these nanomagnets, the inter-element separation is fixed to 50 nm. We have used electron beam lithography processes in order to pattern the nanomagnet chain. The magnetic film (Permalloy: $\text{Ni}_{80}\text{Fe}_{20}$) was then deposited using the e-beam evaporation technique at a base pressure of 2×10^{-8} Torr followed by metal liftoff. Subsequently, a ground-signal-ground (GSG) type CPW is patterned on top of the nanowire using e-beam lithography, and we have deposited 80-nm-thick Pt using the sputtering technique. An adhesive 5-nm-thick Cr layer was deposited using e-beam evaporation before depositing the Pt film. The larger contact pads for the CPW were prepared by using the optical lithography technique followed by thin film deposition of Cr(5 nm)/Pt(200 nm) and metal liftoff. The scanning electron microscopy image of the sample is shown in Fig. 1(b). The dot in Fig. 1(b) represents the nominal size of the laser spot, which is approximately 250 nm.²¹ The length, width, and thickness of each nanomagnet are 600 nm, 260 nm, and 25 nm, respectively. The angle of the slanted edge is 32° . We have used picoprobes in order to connect the CPW to a microwave generator (up to 20 GHz). The CPW is designed to have an impedance of 50 Ω . The width (d) of the signal line of the CPW is $1\ \mu\text{m}$, which limits the maximum wavevector excitation to $2\pi/d = 6.2\ \text{rad}/\mu\text{m}$ (Ref. 22).

Prior to any experiment on spin wave propagation, we have first stabilized a remanent state where all the nanomagnets point in the same direction. Such a remanent magnetic orientation is obtained by simply applying a magnetic field along the x-axis or the y-axis followed by the removal of that field. We recorded BLS spectra at the laser spot position as shown in Fig. 1(b). In order to investigate the microwave power required to gate the SW propagation, we have first increased the microwave power to a certain value [hereby referred to as initializing microwave power ($P_{init.}$)] and subsequently recorded the BLS spectrum by exciting SWs at a certain microwave power [hereby referred to as excitation power ($P_{exc.}$)]. Prior to setting a new value for $P_{init.}$, we have restored the remanent magnetic state by using an external magnetic field. Figure 2(a) shows the BLS intensity as a function of

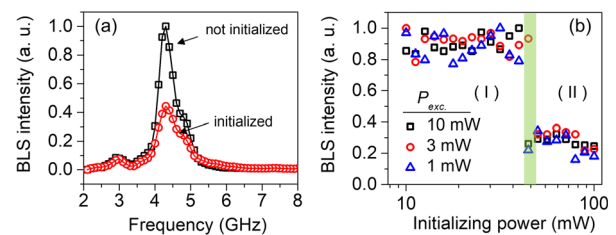


FIG. 2. (a) BLS spectra measured at an excitation power of 1 mW without any microwave power initialization (labeled as not initialized) and with high initializing microwave power (100 mW) (labeled as initialized). (b) BLS intensities as a function of different initializing microwave power. Note that the intensity drops at around 45 mW and the two different intensity regions are marked as I and II. The measurements were performed at 4.2 GHz and at three different microwave excitation powers ($P_{exc.} = 10, 3, \text{ and } 1\ \text{mW}$). Each set of data was normalized with respect to their maximum spin wave intensities.

microwave frequency, which was varied in the range of 2 to 20 GHz at a fixed microwave excitation power of $P_{exc.} = 1$ mW. The spectrum, which is obtained without any microwave power initialization (labeled as ‘not initialized’), shows that spin wave propagation occurs in the range of 3 GHz–5 GHz with a maximum intensity at 4.2 GHz. A detailed study of different initializing microwave powers on the BLS intensity is carried out at a distance of $1.5 \mu\text{m}$ from the CPW, and the results are shown in Fig. 2(b). The initializing power was varied from 10 mW to 100 mW. Prior to any recording of the BLS spectrum shown in Fig. 2(b), we have applied the initializing microwave power at 4.2 GHz for a transient period of approximately 2 s using the CPW and microwave generator. Subsequently, the BLS measurements were carried out for three different excitation powers (1 mW, 3 mW, and 10 mW) at 4.2 GHz. Note that each measurement is normalized to its highest intensity in order to account for any fluctuations during the measurements. We have found that the intensity drops significantly (almost by a factor of 2.5) at a minimum microwave annealing power of around 45 mW. For the simplicity of further discussion, the two different intensity levels below and above around 45 mW are denoted as regions I and II, respectively. A typical spectrum in region II is shown in Fig. 2(a), which is labeled by “initialized.” The results indicate that the magnetic states can be recovered after applying the initializing power without damaging the samples permanently. We would like to point here that the values of microwave power, which are mentioned here, are set at the microwave generator, and therefore, the actual power at the sample may show a slightly lower value due to impedance mismatches/losses at different contact positions.

Such a reduction of BLS intensities as mentioned above, was earlier shown when a magnet was switched in the nanowire by using an external magnetic field.¹⁸ In order to investigate the origin of the gating of spin waves, we have carried out a two dimensional scanning of the BLS intensity by raster scanning the laser spot on top of the nanowire. This is achieved by using a nanostage on top of which the nanowire was placed. The sample was raster-scanned in steps of 100 nm along x- and y-directions under the fixed laser spot. The spatial maps of the 4.2 GHz SW mode for regions I and II are shown in Fig. 3. Note that each pixel of the spatial map corresponds to the BLS intensity at 4.2 GHz. Figure 3(a) was obtained by recording BLS intensities at an excitation power of 10 mW without any initialization with microwave

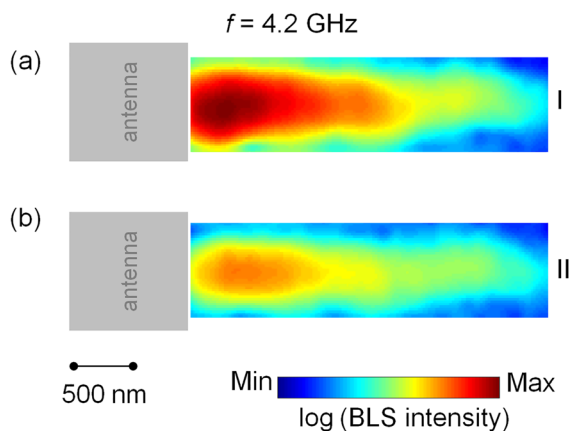


FIG. 3. 2D spatial maps of the 4.2 GHz spin wave mode for (a) region I and (b) region II as shown in Fig. 2.

power. One can see the decay of the SW intensity away from the microwave antenna, which has an exponential decay character: $\exp(-2x/\lambda)$, where λ = decay length. A line scan of the BLS intensity from Fig. 3(a) reveals the value of the decay length to be close to $1 \mu\text{m}$. On the other hand, Fig. 3(b) refers to a state where >45 mW microwave power was used for initialization purposes prior to the recording of the BLS intensities at an excitation power of 10 mW. The BLS intensity is significantly low in Fig. 3(b) as compared to Fig. 3(a). Moreover, the spin wave spatial map is continuous in Fig. 3(b), which suggests that the magnetic states of the nanomagnets away from the antenna are not altered by the initializing microwave power. This is in contrast to our earlier observation of the disappearance of the BLS intensity at the location of the switched nanomagnet, resulting in a discontinuous spin wave spatial profile.¹⁸ Therefore, one may expect any switching events only underneath the CPW where the microwave field is maximum. Note that the microwave field (h_{MW}) direction is along the $\pm x$ axis [Fig. 1(a)]. The corresponding magnetic states for $+x$ and $-x$ field initializations are opposite to each other for the rhomboid nanomagnets as shown in Fig. 1(a) due to the shape induced anisotropy.¹⁹ However, due to the 80-nm-thick CPW, we could not measure spin wave intensities using the BLS laser probe for the nanomagnets under the CPW.

Nevertheless, in order to directly probe the remanent magnetic states, MFM images were recorded for these two different regions (I and II). Prior to the MFM imaging, the sample was initialized by applying a saturating field along the width of the waveguide and subsequently by removing it. This remanent state represents region I. On the other hand, region II is obtained by applying an initializing microwave power of >45 mW prior to MFM imaging. The results are shown in Fig. 4. We do not observe any difference in the magnetic configurations on the left or right of the CPW. This is consistent with the 2D spatial map of 4.2 GHz mode. The MFM results further suggest that the magnetic orientation of the nanoelements underneath the CPW must have been modified upon microwave power annealing. Note that it is difficult to probe 25-nm-thick nanomagnets using MFM, which are underneath a thick antenna [Cr(5 nm)/Pt(80 nm)]. However, we do see clear differences in the MFM contrasts underneath the CPW between Figs. 4(a) and 4(b). The three nanomagnets underneath the CPW can be clearly seen from the SEM image of the nanowire [Fig. 1(b)]. One can observe bright MFM contrasts on top for all the three nanomagnets underneath the CPW like the rest of the nanomagnets as shown in Fig. 4(a). In contrast, Fig. 4(b) does not

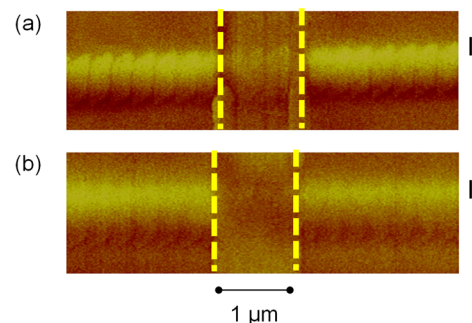


FIG. 4. MFM images showing the magnetic ground states for (a) region I and (b) region II, as shown in Fig. 2.

show all bright contrasts on top for these three nanomagnets. This indicates that the nanomagnets underneath the CPW have been switched. We have repeated the experiments several times, and the results, as shown in Fig. 4, are reproducible. We would like to point here that we have used an external magnetic field in order to restore the original magnetic configuration by applying an initialization field along the +x-direction prior to each measurement. It will be of future interest to reconfigure these nanomagnets using a DC pulsed current through the same CPW, which will enable on-chip gating in a magnonic device. Also, note here that microwave assisted switching, which is being exploited in magnetic storage, occurs on the sub- μs timescale.²³ It is much smaller than the time (2 s) that is used here for initializing microwave power. Therefore, this report stimulates further experiments with microwave pulse trains for initialization in order to explore the minimum pulse duration required for spin wave gating.

We would like to emphasize the difference of this present demonstration with respect to our earlier work.¹⁸ In our earlier study, we have demonstrated gating or manipulation of SW signals by switching one of the nanomagnets in the nanowire and we showed that the BLS intensity significantly drops due to the switched magnet in the nanowire away from the antenna. An oppositely oriented nanomagnet was lithographically prepared away from the excitation antenna for gating of SW propagation in this earlier work. It requires additional lithographic processes for additional contact pads in order to realize such a gating operation. This is in sharp contrast to the present demonstration where no magnets are specifically fabricated using lithography, i.e., all the nanomagnets in the wire are physically similar to each other. Rather, we have used the same CPW as both an input and a gate for excitation and manipulation of spin waves [Fig. 1(b)]. Thus, it reduces the number of lithographic steps by totally removing the need of a separate gate terminal.

We have shown gating of spin waves using microwave power in a nanowire based on dipolar coupled nanomagnets. The micro-BLS technique is used to directly image spin waves at different positions on the nanowire in order to study spin wave propagation characteristics. Critical microwave power required for spin wave gating was found from systematic micro-BLS measurements at different initializing microwave powers, and it is found to be around 45 mW. Furthermore, combination of the 2D spatial profile of the spin wave mode and MFM images indicates that the switching of the nanomagnets underneath the CPW is behind the origin of the SW gating. The results are promising for the realization of on-chip spin wave manipulation, which is of great demand for device integration.

A.H. would like to thank the funding under the early career research award SERB (No. ECR/2017/000571) and Ramanujan Fellowship (No. SB/S2/RJN-118/2016), Department of Science and

Technology (DST), India. A.O.A would like to acknowledge funding from the Wolfson Foundation and Royal Society through the Royal Society Wolfson Fellowship.

The data that support the findings of this study are available within this article.

REFERENCES

- ¹See https://www.semiconductors.org/wp-content/uploads/2018/06/0_2015-ITRS-2.0-Executive-Report-1.pdf for “International Technology Roadmap for Semiconductors 2.0 (2015 Edition), Executive Report, 2015.”
- ²D. Grundler, *Nat. Phys.* **11**, 438–441 (2015).
- ³A. V. Chumak, V. I. Vasyuchka, A. A. Serga, and B. Hillebrands, *Nat. Phys.* **11**, 453–461 (2015).
- ⁴D. Sander, S. O. Valenzuela, D. Makarov, C. H. Marrows, E. E. Fullerton, P. Fischer, J. McCord, P. Vavassori, S. Mangin, P. Pirro, B. Hillebrands, A. D. Kent, T. Jungwirth, O. Gutfleisch, C. G. Kim, and A. Berger, *J. Phys. D* **50**, 363001 (2017).
- ⁵B. Lenk, H. Ulrichs, F. Garbs, and M. Münzenberg, *Phys. Rep.* **507**, 107–136 (2011).
- ⁶M. Madami, S. Bonetti, G. Consolo, S. Tacchi, G. Carlotti, G. Gubbiotti, F. B. Mancoff, M. A. Yar, and J. Akerman, *Nat. Nanotechnol.* **6**, 635–638 (2011).
- ⁷V. E. Demidov, S. Urazhdin, and S. O. Demokritov, *Nat. Mater.* **9**, 984–988 (2010).
- ⁸M. P. Kostylev, A. A. Serga, T. Schneider, B. Leven, and B. Hillebrands, *Appl. Phys. Lett.* **87**, 153501 (2005).
- ⁹T. Schneider, A. A. Serga, B. Leven, B. Hillebrands, R. L. Stamps, and M. P. Kostylev, *Appl. Phys. Lett.* **92**, 022505 (2008).
- ¹⁰K.-S. Lee and S.-K. Kim, *J. Appl. Phys.* **104**, 053909 (2008).
- ¹¹V. E. Demidov, S. Urazhdin, and S. O. Demokritov, *Appl. Phys. Lett.* **95**, 262509 (2009).
- ¹²A. Khitun, M. Bao, and K. L. Wang, *J. Phys. D* **43**, 264005 (2010).
- ¹³A. V. Chumak, A. A. Serga, and B. Hillebrands, *Nat. Commun.* **5**, 4700 (2014).
- ¹⁴M. Vogel, A. V. Chumak, E. H. Waller, T. Langner, V. I. Vasyuchka, B. Hillebrands, and G. von Freymann, *Nat. Phys.* **11**, 487–491 (2015).
- ¹⁵K. Wagner, A. Kákay, K. Schultheiss, A. Henschke, T. Sebastian, and H. Schultheiss, *Nat. Nanotechnol.* **11**, 432–436 (2016).
- ¹⁶E. Albisetti, D. Petti, M. Pancaldi, M. Madami, S. Tacchi, J. Curtis, W. P. King, A. Papp, G. Csaba, W. Porod, P. Vavassori, E. Riedo, and R. Bertacco, *Nat. Nanotechnol.* **11**, 545–551 (2016).
- ¹⁷J. Topp, D. Heitmann, M. P. Kostylev, and D. Grundler, *Phys. Rev. Lett.* **104**, 207205 (2010).
- ¹⁸A. Haldar, D. Kumar, and A. O. Adeyeye, *Nat. Nanotechnol.* **11**, 437–443 (2016).
- ¹⁹A. Haldar and A. O. Adeyeye, *ACS Nano* **10**, 1690–1698 (2016).
- ²⁰T. Sebastian, K. Schultheiss, B. Obry, B. Hillebrands, and H. Schultheiss, *Front. Phys.* **3**, 35 (2015).
- ²¹S. O. Demokritov and V. E. Demidov, *IEEE Trans. Magn.* **44**, 6–12 (2008).
- ²²V. E. Demidov, M. P. Kostylev, K. Rott, P. Krzysteczko, G. Reiss, and S. O. Demokritov, *Appl. Phys. Lett.* **95**, 112509 (2009).
- ²³S. Okamoto, N. Kikuchi, M. Furuta, O. Kitakami, and T. Shimatsu, *J. Phys. D* **48**, 353001 (2015).